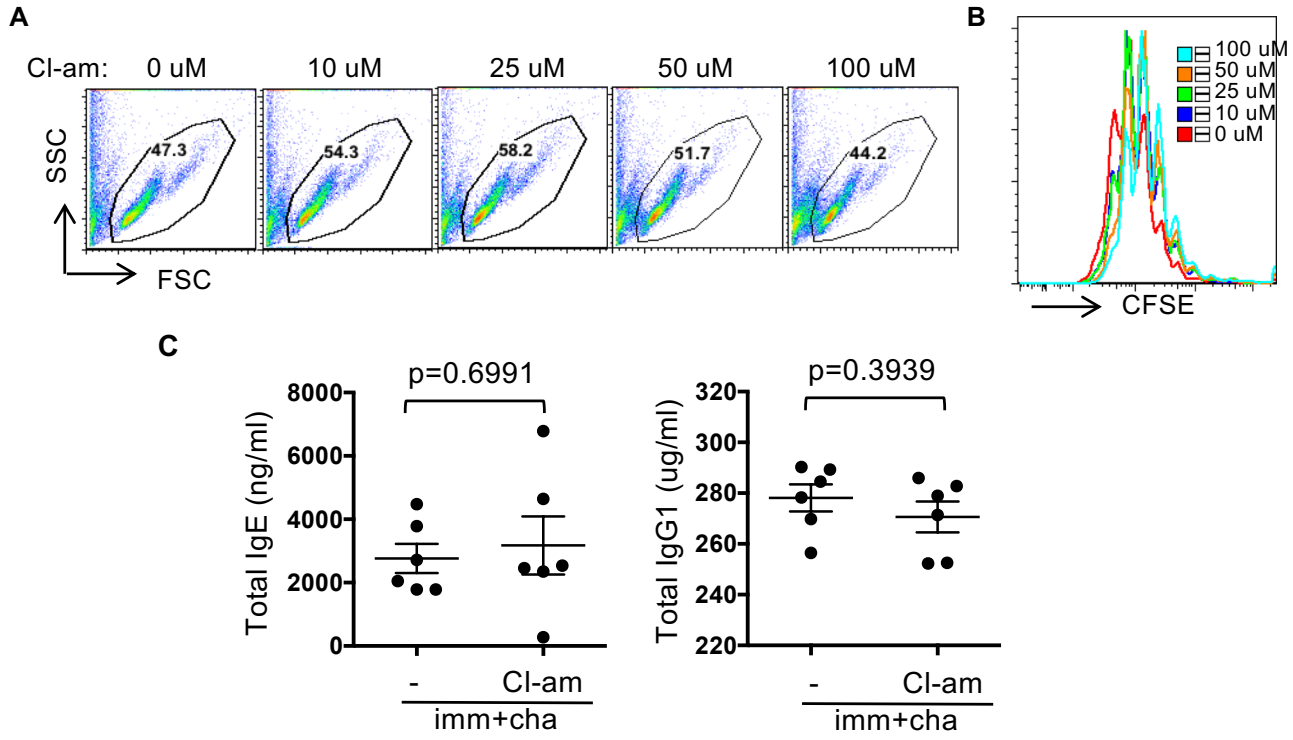

Supplemental Figure 1: Negligible impact of Cl-am on the activation/proliferation of Th cells and the serum level of total IgE or IgG1. Th cells of C57BL/6 mice were stained with CFSE and stimulated in vitro with anti-CD3/anti-CD28/IL-2 in the presence of Cl-am of indicated concentration for 3 days. The FSC/SSC (**A**) and dilution of CFSE (**B**) were analyzed with FACS (N=2). Total serum IgE and IgG1 from mice described in Figure 1E-1H is shown in **C**.

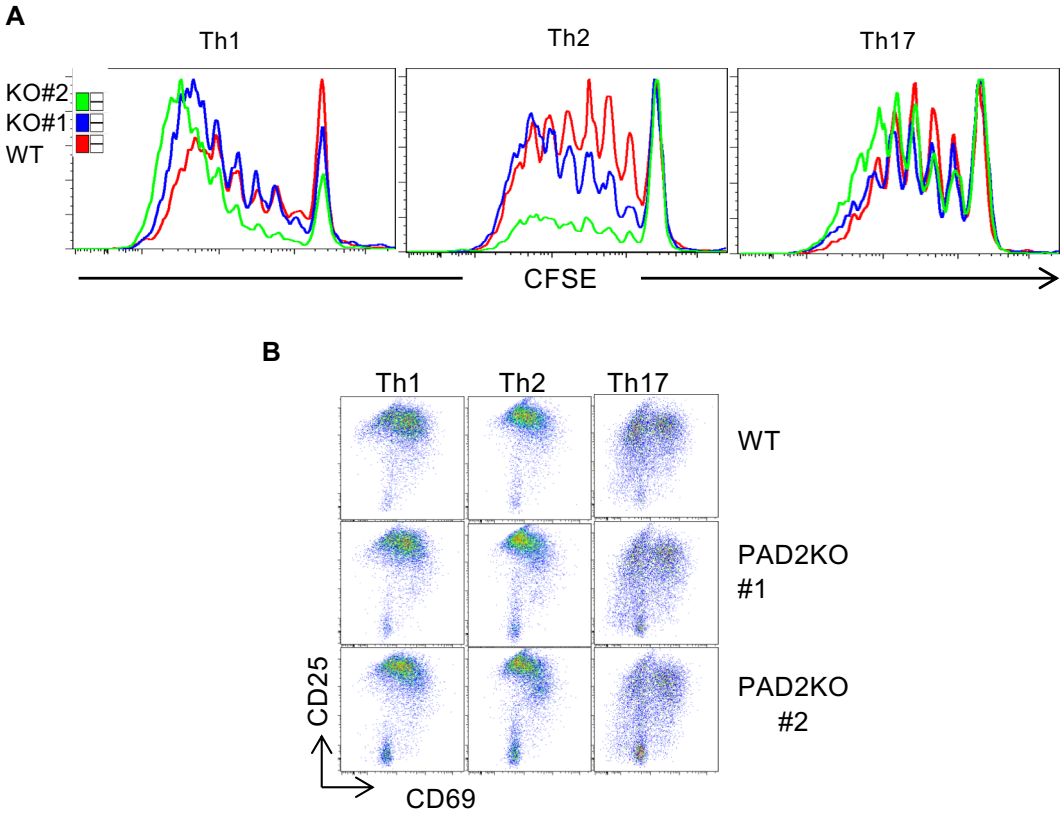

Supplemental Figure 2. Deficiency of PAD2 had little impact on the proliferation and activation of Th cells. WT DBA/1J and PAD2KO Th cells were stained with CFSE and differentiated into Th1, Th2 and Th17 cells. The dilution of CFSE (**A**) and the level of CD69 and CD25 (**B**) were analyzed with FACS three days after the initial stimulation.

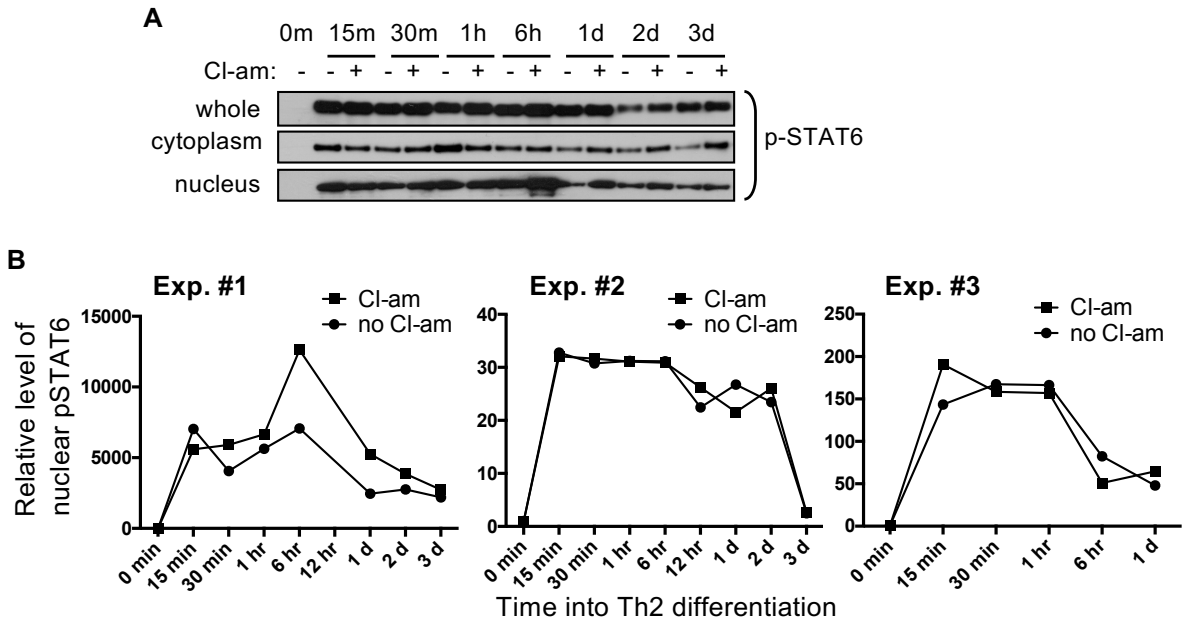

Supplemental Figure 3. Kinetics of STAT6 phosphorylation in differentiating Th2 cells. Th cells of C57BL/6 mice were stimulated under Th2-polarizing conditions in the absence (-) or presence (+) of 50 uM Cl-am. Whole cell, cytoplasmic and nuclear extract were prepared at indicated time points and the levels of phosphorylated STAT6 (pSTAT6) were analyzed by western blotting. Representative western blots from three experiments are shown in **A**. The density of nuclear pSTAT6 was quantified with ImageJ program. The density at time 0 was arbitrarily set at 1. m stands for minute; h for hour; and d for day. The normalized density of nuclear pSTAT6 from three independent experiments are shown in **B**.

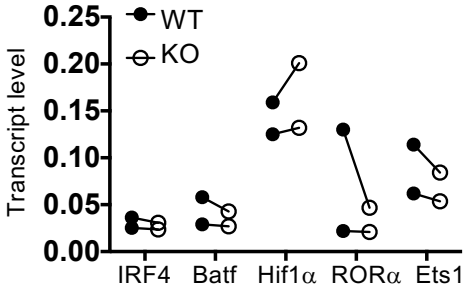

Supplemental Figure 4. Expression of other transcription factors in Th17 cells. WT DBA/1J and PAD2KO Th cells were differentiated into Th17 cells for 5 days. The transcript levels of indicated transcription factors were measured with real time PCR and normalized against that of actin. Data points from the same experiments are connected with line.

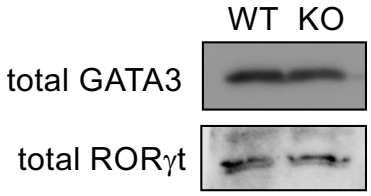

Supplemental Figure 5: Levels of GATA3 and RORγt proteins in nuclear extract used in Fig. 5I and 5J. The amount of GATA3 or RORγt proteins used in each EMSA reaction shown in Figure 5I an 5J was quantified with western blotting using anti-GATA3 or anti-RORγt.

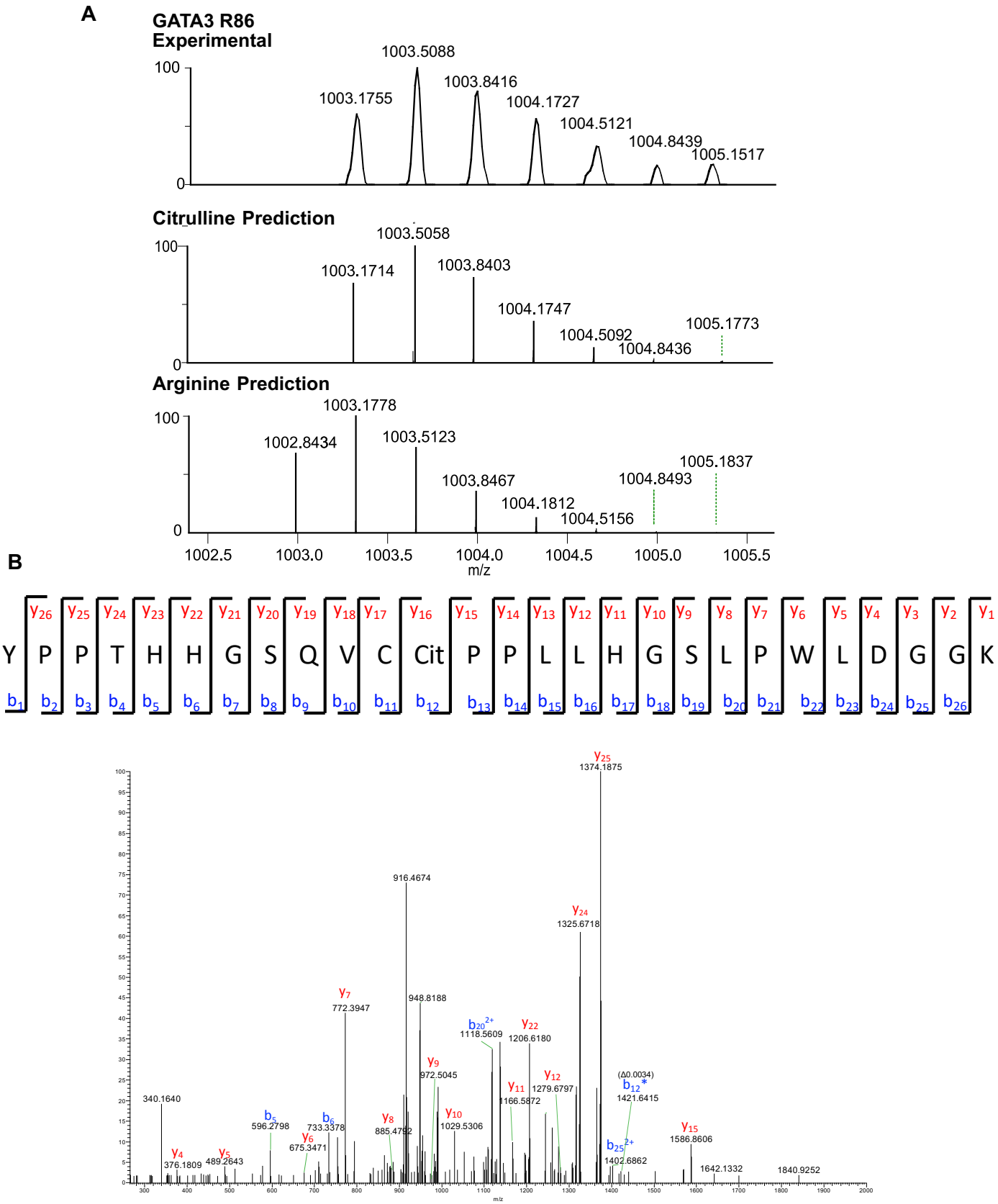

Supplemental Figure 6. Mass spectrometry analysis of GATA3 R86 fragment Ion. A. MS1 isotopic envelope (FTMS) compared to a predicted citrulline and arginine ion showing a citrulline match. **B.** MS2 (FTMS) of citrulline-containing peptide, with b and y ions annotated, showing the expected mass shift (*) on the citrulline fragment.

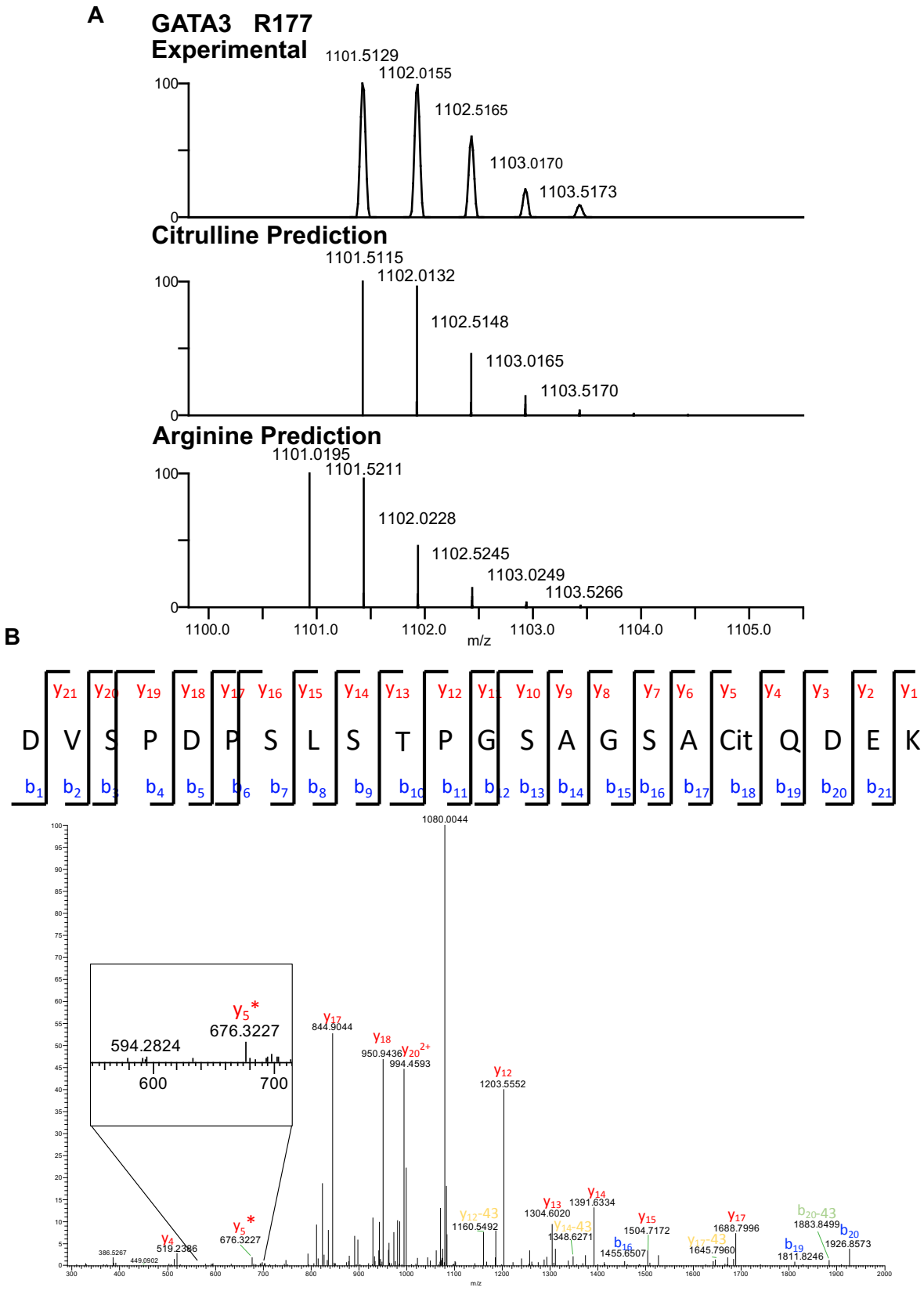

Supplemental Figure 7: Mass spectrometry analysis of GATA3 R177 fragment Ion. A. MS1 isotopic envelope (FTMS) compared to a predicted citrulline and arginine ion showing a citrulline match. **B.** MS2 (FTMS) of citrulline-containing peptide, with b and y ions annotated, showing the expected mass shift (*) on the citrulline fragment alongside multiple neutral loss (-43 Da) ions.

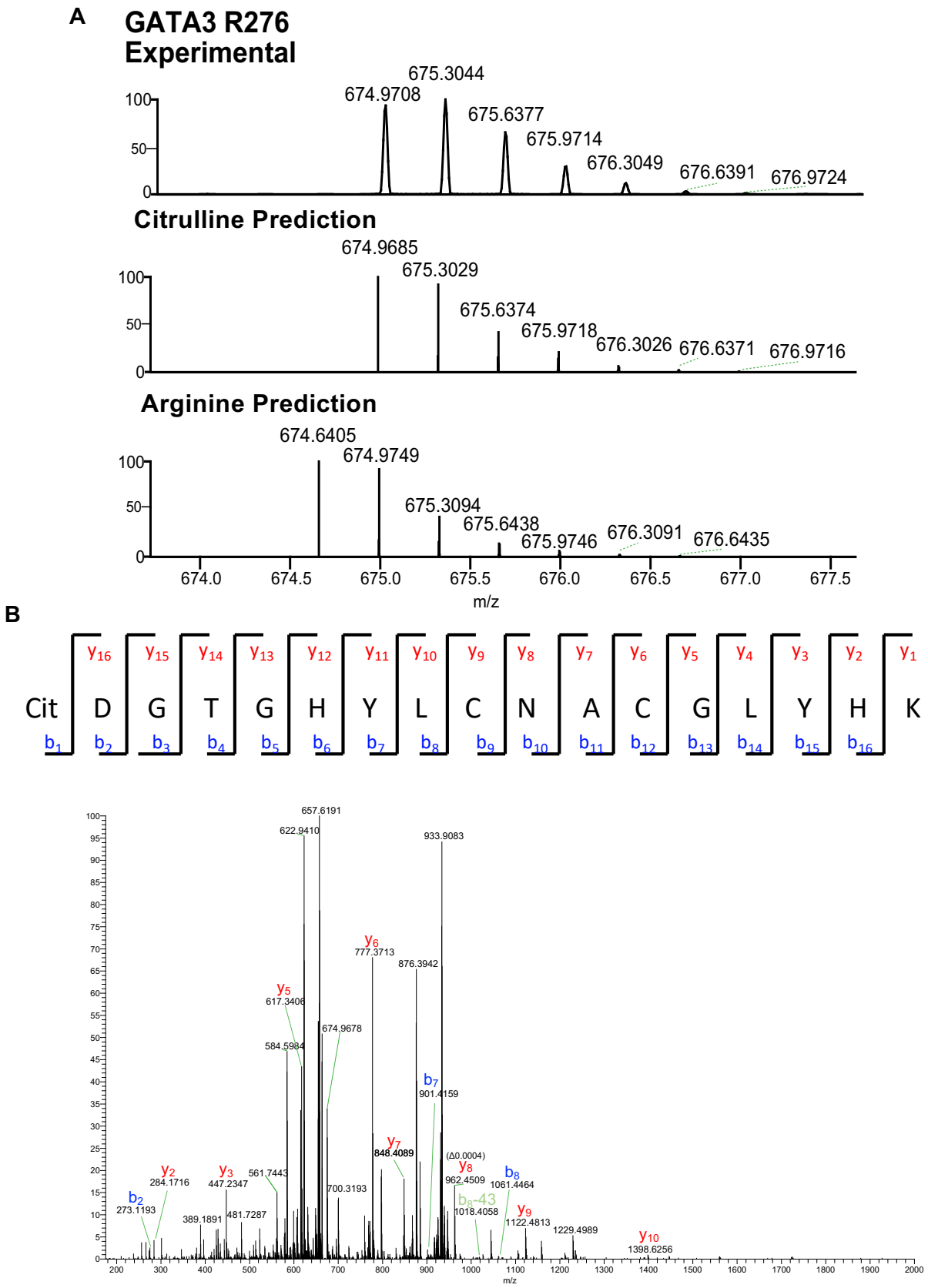

Supplemental Figure 8: Mass spectrometry analysis of GATA3 R276 Fragment Ion. A. MS1 isotopic envelope (FTMS) compared to a predicted citrulline and arginine ion showing a citrulline match. **B.** MS2 (FTMS) of citrulline-containing peptide, with b and y ions annotated, showing a neutral loss (-43 Da) on a citrulline-containing fragment.

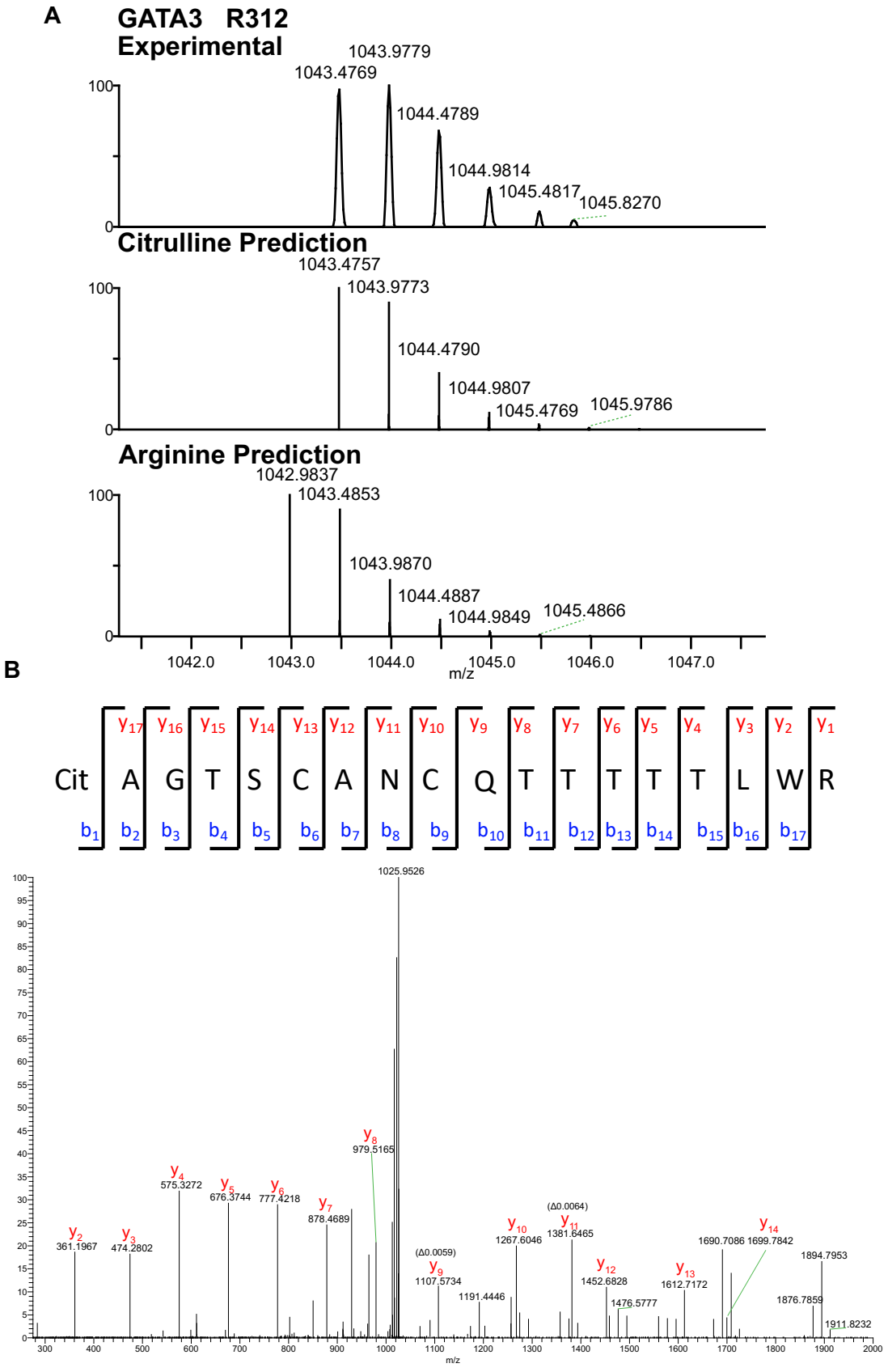

Supplemental Figure 9: Mass spectrometry analysis of GATA3 R312 Fragment Ion. A. MS1 isotopic envelope (FTMS) compared to a predicted citrulline and arginine ion showing a citrulline match. **B.** MS2 (FTMS) of citrulline-containing peptide ions annotated. The mass of the Gln and Asn fragment ions do not indicate a +0.984 Da indicative of deamination.

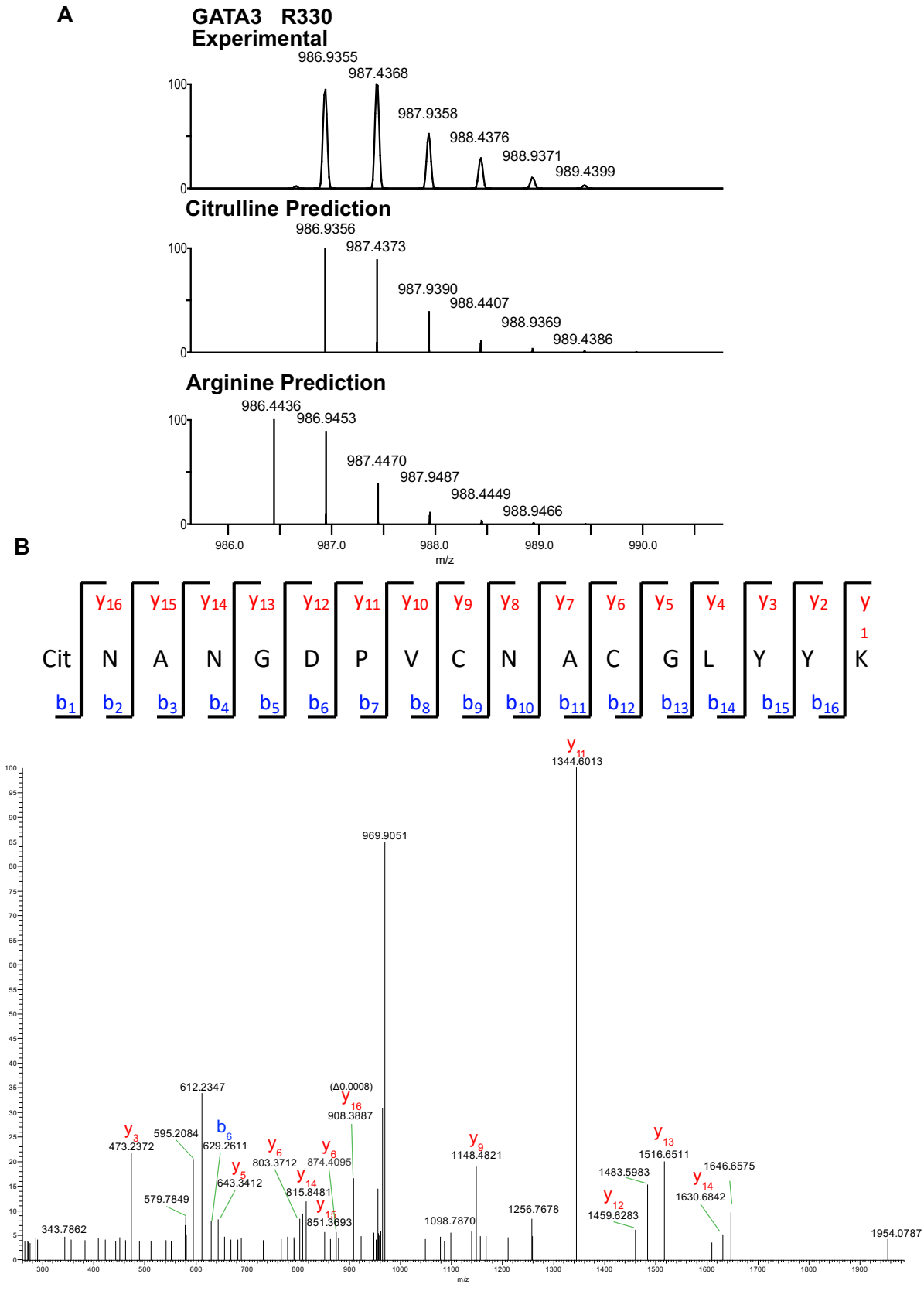

Supplemental Figure 10: Mass spectrometry analysis of GATA3 R330 Fragment Ion. A. MS1 isotopic envelope (FTMS) compared to a predicted citrulline and arginine ion showing a citrulline match. **B.** The data shown here is the MS2 (FTMS) of citrulline-containing peptide, with b and y ions annotated. While the common criteria is lacking, y_{16} is accurate, therefore the mass shift must be from a citrulline.

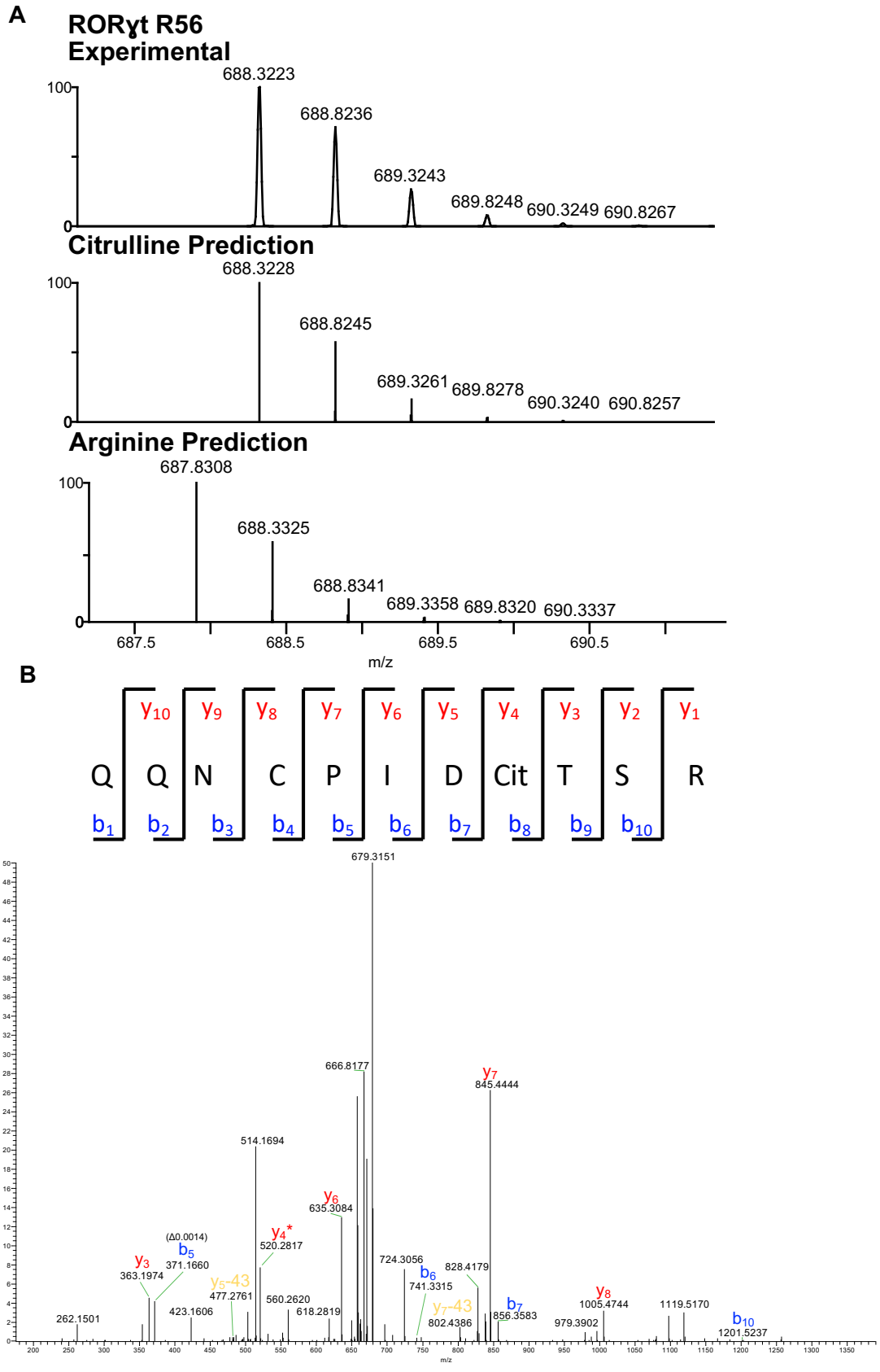

Supplemental Figure 11: Mass spectrometry analysis of RORγt R56 Fragment Ion. A. MS1 isotopic envelope (FTMS) compared to a predicted citrulline and arginine ion showing a citrulline match. **B.** MS2 (FTMS) of citrulline-containing peptide, with b and y ions annotated, showing the expected mass shift (*) on the citrulline fragment alongside multiple neutral loss (-43 Da) ions.

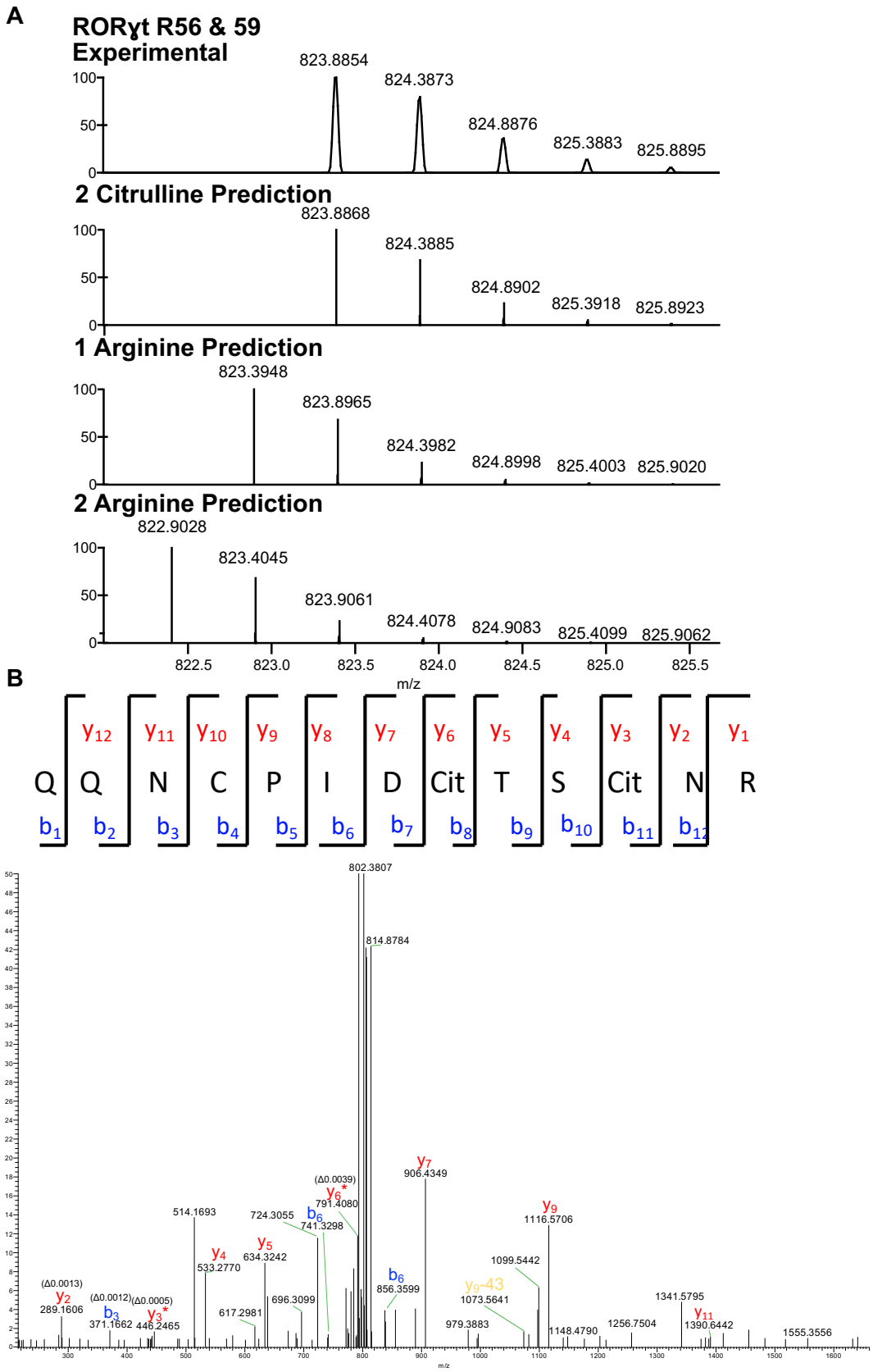

Supplemental Figure 12: Mass spectrometry analysis of RORγt R56 and R59 Fragment Ion. A. MS1 isotopic envelope (FTMS) compared to a predicted citrulline and arginine ion showing a citrulline match. **B.** MS2 (FTMS) of citrulline-containing peptide, with b and y ions annotated, showing the expected mass shift (*) on the citrulline fragment alongside multiple neutral loss (-43 Da) ions.

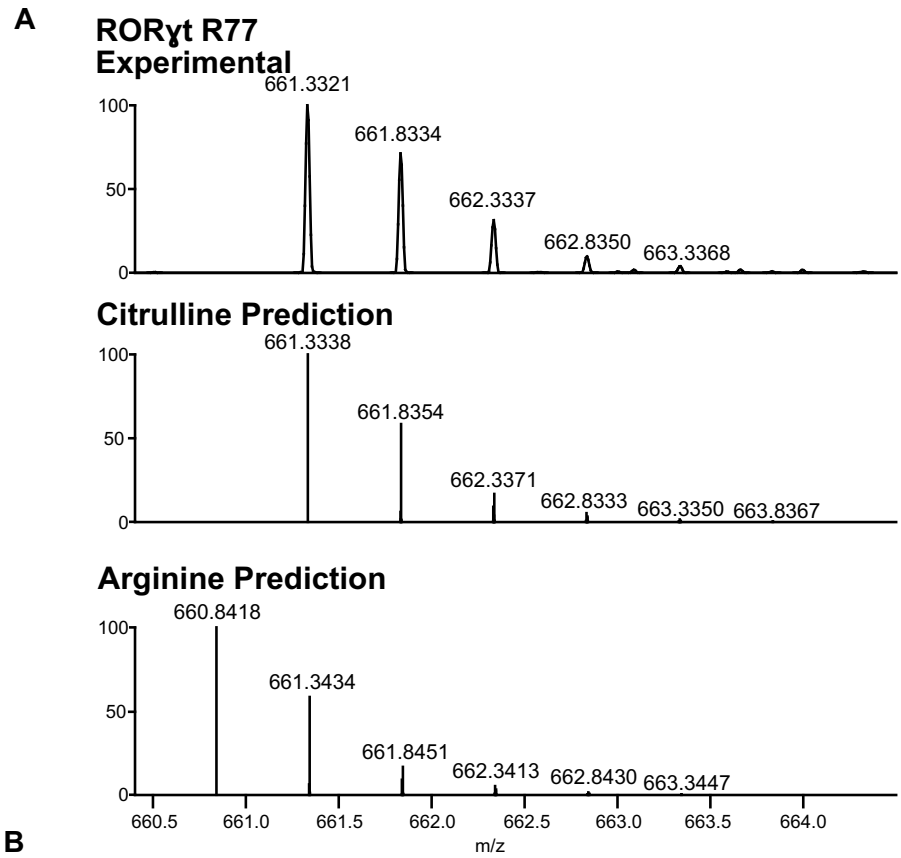

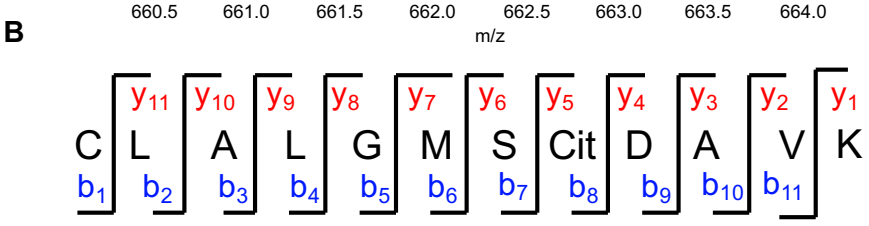

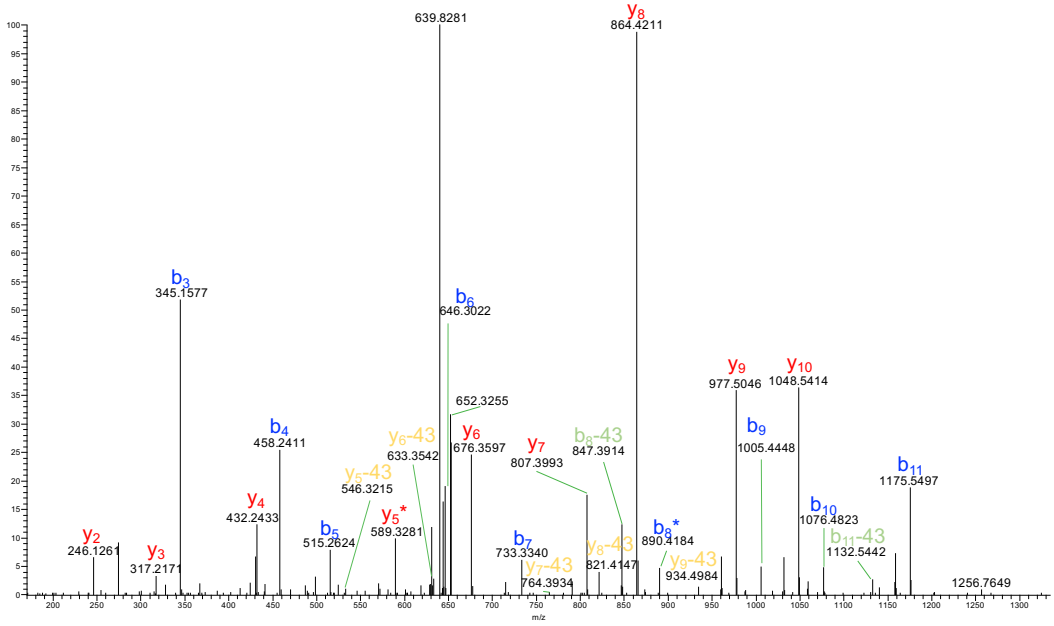

Supplemental Figure 13: Mass spectrometry analysis of RORγt R77 Fragment Ion. A. MS1 isotopic envelope (FTMS) compared to a predicted citrulline and arginine ion showing a citrulline match. **B.** MS2 (FTMS) of citrulline-containing peptide, with b and y ions annotated, showing the expected mass shift (*) on the citrulline fragment alongside multiple neutral loss (-43 Da) ions.

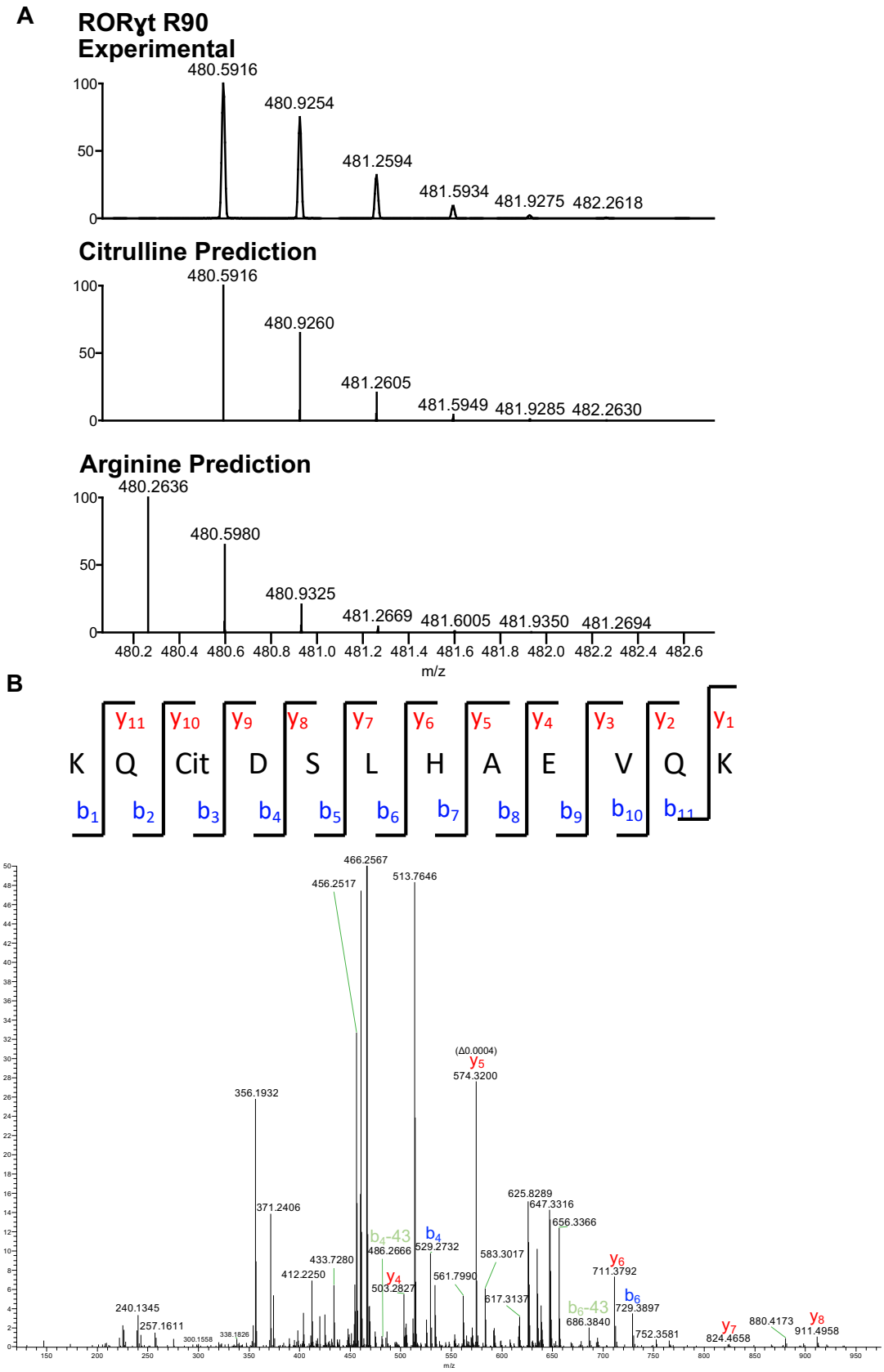

Supplemental Figure 14: Mass spectrometry analysis of RORγt R90 Fragment Ion. A. MS1 isotopic envelope (FTMS) compared to a predicted citrulline and arginine ion showing a citrulline match. **B.** MS2 (FTMS) of citrulline-containing peptide, with b and y ions annotated, showing the expected mass shift (*) on the citrulline fragment alongside multiple neutral loss (-43 Da) ions.

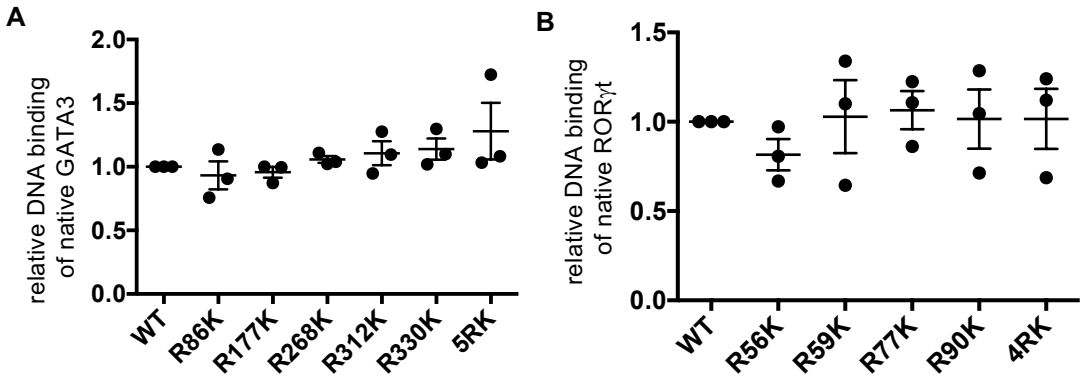

Supplemental Figure 15. The R-to-K mutations do not affect the DNA binding of native GATA3 and RORγt. Native recombinant GATA3 (**A**), RORγt (**B**), and their R-to-K mutants were used in EMSA as in Figure 6. The density of the shifted probes was quantified with ImageJ program. The density of WT GATA3- or WT RORγt-sifted probes was arbitrarily set as 1. Each dot represents one data point from a total of three experiments.

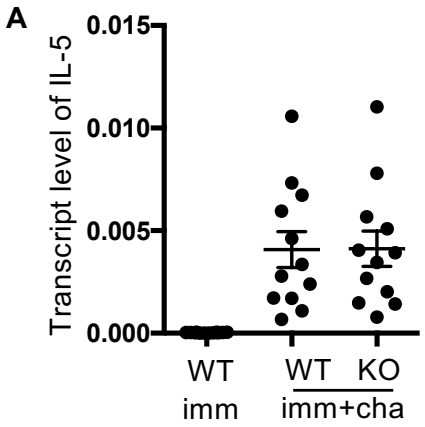

Supplemental Figure 16. Induction of allergic airway inflammation. The transcript levels of IL-5 in the lungs from mice described in Figure 8A-8G are shown.

Supplemental Table 1. Citrullinated peptides identified with tandem mass spectrometry

Protein	Residue	Peptide	charge	Calculated Mass	
				(Citrulline)	Observed Mass
GATA3	86	YPPTHHGSQVCR*PPLLHGSLPWLDGGK	3	1003.1714	1003.1755
	177	DVSPDPSLSTPGSAGSAR*QDEK	2	1101.5115	1101.5129
	276	R*DGTGHYLCNACGLYHK	3	674.9698	675.9708
	312	R*AGTSCANCQTTTTTLWR	2	1043.4757	1043.4769
	330	R*NANGDPVCNACGLYYK	2	986.9356	986.9355
RORγt	56	QQNCPIDR*TSR	2	688.3228	688.3223
	59	QQNCPIDR*TSR*NR	2	823.8868	823.8854
	77	CLALGMSR*DAVK	2	661.3338	661.3321
	90	KQR*DSLHAEVQK	3	480.5916	480.5916

R* represents peptidylcitrulline

Supplemental Table 2: The sequences of the primers used in qPCR

gene	forward primer	reverse primer
mouse PAD1	5'-TGTGTGCGTGGTAGGTGTG-3'	5'-TCGAGGGATCGTAGACCATGT-3'
mouse PAD2	5'-CTGTTTCCCCGACGAGAGTTT-3'	5'-ACACAGGAGGCAAGATGTTGG-3'
mouse PAD3	5'-TGTTTGAGGTCTACGGGACAC-3'	5'-GGTCATTGCTAGGGGAGTTCA-3'
mouse PAD4	5'-TCTGCTCCTAAGGGCTACACA-3'	5'-GTCCAGAGGCCATTTGGAGG-3'
mouse PAD6	5'-TGGTAGGCATGGAAATCACCT-3'	5'-GCAGGAGCTAGAGATGTGGAT-3'
mouse IFN-γ	5'- CGGCACAGTCATTGAAAGCCTA-3'	5'- GTTGCTGATGGCCTGATTGTC-3'
mouse IL-4	5'- CGAATGTACCAGGAGCCATATC-3'	5'- TCTCTGTGGTGTTCTTCGTTG-3'
mouse IL-5	5'- AGATTCCCATGAGCACAGTG-3'	5'- TGTCTAGCCCCTGAAAGATTTC-3'
mouse IL-13	5'- AGGAGCTGAGCAACATCAC-3'	5'- GGGTCCTGTAGATGGCATTG-3'
mouse IL-17A	5'-AGGCAGCAGCGATCATCC-3'	5'-TGGAACGGTTGAGGTAGTCTG-3'
mouse IL-17F	5'-TGCTACTGTTGATGTTGGGAC-3'	5'-AATGCCCTGGTTTTGGTTGAA-3'
mouse GATA3	5'-CTCGGCCATTCGTACATGGAA-3'	5'-GGATACCTCTGCACCGTAGC-3'
mouse RORγt	5'-GACCCACACCTCACAAATTGA-3'	5'-AGTAGGCCACATTACACTGCT-3'
mouse actin	5'- GGCTGTATTCCCCTCCATCG -3'	5'- CCAGTTGGTAACAATGCCATG -3'
mouse HPRT	5'-AGTACAGCCCCAAAATGGTTAAG-3'	5'- CTTAGGCTTTGTATTTGGCTTTTC-3'